Flow patterns and optimization of compartments for the anaerobic baffled reactor

Ming Xu, Lili Ding, Ke Xu, Jinju Geng, Hongqiang Ren*

State Key Laboratory of Pollution Control and Resource Reuse, School of the Environment, Nanjing University, Nanjing 210093, Jiangsu, P.R. China, Tel. +86 25 89680512; Fax: +86 25 89680569; email: hqren@nju.edu.cn (H. Ren)

ABSTRACT

The anaerobic baffled reactor (ABR) possesses many advantages such as high removal efficiency, outstanding working stability, and lower operating cost. In this essay, four reactors of equal effective volume (56.4 L) that were designed with three, four, five, and six compartments were adopted to investigate the flow patterns of the ABR through the tracer pulse stimulus-response technique and cold-model tests. The dead space decreases with the increase in the ABR compartments; specifically, the mean dead space induced by biomass and hydraulic behavior in 3-, 4-, 5-, and 6-compartment ABRs were 6.40, 5, 3.30, and 3%, respectively. In addition, the increase in ABR compartments also resulted in the decrease in back-mixing and 1/Pez values (from 0.118 to 0.060), which made the fluid in the reactor approach to the plug flow state. Analysis of the theoretical optimal number of ABR compartments shows that, the series number (N) of compartments shall be kept at $4 \leq N \leq 5$ when the removal efficiency of the reaction system is 50% and $4 \leq N \leq 6$ when the removal efficiency of the reaction system is 90%. Taking the operating performance and economic factors of the reactor into full consideration, the present study recommends that the series number (N) of ABR compartments shall be kept at 4 or 5.

Keywords: Anaerobic baffled reactor; Flow pattern; Back-mixing; Dead space; Volumetric efficiency

1. Introduction

Anaerobic digestion technology has lot of advantages, such as high COD removal efficiency, high system stability, no requirement for aeration, and larger biomass retention [1–4]. Therefore, the reactors that adopt anaerobic digestion technology are widely applied in both environmental engineering and energy engineering [5–10].

The anaerobic baffled reactor (ABR), which belongs to the third generation high-rate anaerobic reactor, is highly appraised for its high efficiency, outstanding working stability, and lower operating cost [11,12]. It is generally composed of an up-flow anaerobic sludge blanket and a staged multi-phase anaerobic digestion [13]. Such a design realizes microbial alternation in the different compartments along the flow direction

---

*Corresponding author.

[14–16]; it also achieves high-effective separation of acid and methanogenic microbes, and transforms the whole reaction system from one single-phase into two- or multi-phase process [17–19].

Ghaniyari-Benis et al. [20] adopted the multistage biofilm reactor to treat the synthetic medium-strength wastewater. Their results indicated that efficiencies of the multistage biofilm reactor in removing COD reached 91.6, 91.6, 90, and 88.3%, respectively, when its organic loading rates were set at 3, 4.5, 6.75, and 9.0 kg COD/m^3 d, accordingly. The effect of toxic shock was also investigated in their research and results showed that the main advantage of using this bioreactor lied in its compartmentalized structure. In another research, Ghaniyari-Benis et al. [21] used the multistage biofilter to treat high-strength wastewater. The results showed that denitrification took place almost solely in the first three compartments of the reactor, with efficiencies at 85, 95, and 98%, respectively. In addition, the denitrification also caused an increase in the total volume of produced biogas from 102 to 178 L/d. By contrast, the ABR designed in our study was mainly adopted to realize controllable hydrolysis and acid genesis; it showed no significant effect in biogas production.

Recently, the ABR has been widely used in the treatment of printing and dyeing wastewater [22,23], hyper saline wastewater [24], nitrobenzene wastewater [25], municipal food waste [26], and wastewater caused by H_2 production [27,28].

The flow patterns of the reactor greatly influence back-mixing, dead spaces, and volumetric efficiency of the reactor [29], which consequently affects treatment efficiency, working stability, reaction time, and equipment investment [4]. A good flow pattern promotes the substrate transferring to microorganisms, maintains uniformity of environmental factors thereby assuring the effective use of the reactor volume by preventing stratification (solid deposition and scum

formation) [30–33]. Therefore, it is imperative to understand and assess the performance of the flow patterns of the ABR and the correlation between the flow pattern and back-mixing, dead spaces and volumetric efficiency so that the engineering application of the ABR can be more efficiently realized.

Tracer experiments are often conducted to estimate the residence time distribution (RTD) [34–37], the time distribution for particles entering and leaving the system. Therefore, RTD curves obtained from tracer tests can be employed to analyze the flow patterns. The present study aims to characterize flow patterns of the ABR through RTD curves, the axial dispersion model and the tank-in-series model.

2. Materials and methods

2.1. Experimental set-up

The laboratory scale reactor used in this experimental study was constructed with plexiglass (Fig. 1), with external dimensions of 64.5, 25, and 40 cm for length, width, and depth, respectively. It consisted of five symmetric compartments and the total working volume of each compartment is 11.3 L or 56.4 L. Each compartment was comprised of an influent inlet port and an exit port. The hanging baffles which were designed in the compartments of the ABR divided each compartment into a down-flow section and an up-flow section. In the present study, four reactors of the same effective volume were designed with three, four, five, six compartments, respectively (Table 1). Both the inlet and outlet pipe were 15 mm in diameter, with the flow rate at 2 L/h. A physical model of the 5-compartment ABR was also designed and then calibrated through measured values of the RTD curve. The total number of grid points in the computational domain of the 5-compartment ABR was 119, 172 (Fig. 2). The COD/-BOD_5 ratios from the first to fifth compartments were
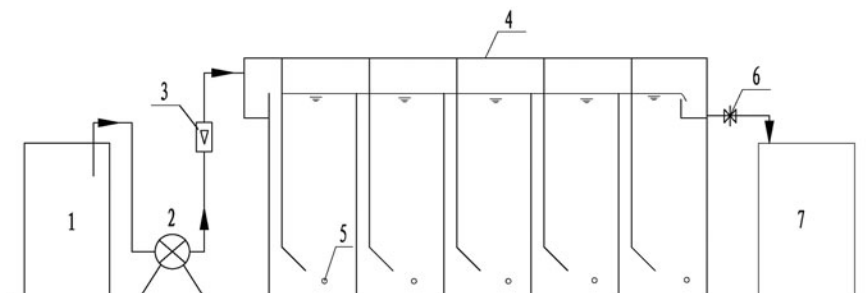
Fig. 1. The schematic diagram of experimental setup (1. influent tank, 2. peristaltic pump, 3. wastewater meter, 4. ABR, 5. mud valve, 6. effluent valve, and 7. effluent tank).

Table 1
Basic physical parameters of the ABR

ABR compartment index	Length (cm)	Width (cm)	Height (cm)	Volume available (L)	Compartment volume (L)	Upflow/ downflow ratio
3-Compartment ABR	64.5	25	40	56.4	18.8	4:1
4-Compartment ABR	64.5	25	40	56.4	14.1	4:1
5-Compartment ABR	64.5	25	40	56.4	11.28	4:1
6-Compartment ABR	64.5	25	40	56.4	9.4	4:1

2.97, 3.16, 3.10, 2.91, and 2.42, respectively. The COD:N:P ratio was 100:5:1. The VFA concentrations of each compartment from the first to fifth compartments were 5.5, 4.8, 4.2, 3.4, and 2.5 mmol/L, respectively.z

2.2. Experimental design

In the present study, the tracer was pulsively injected ($t = 0$) at the tracer injection point of the ABR. Its concentration was measured at the tracer collection point (Fig. 1). The exit time distribution for a pulse input could be used to indicate the RTD of the fluid, $E(t)$. A solution containing 72.5 mg KCl (34.5 mg Cl$^-$) was used as the tracer and was applied during each tracer run, wherein the tracer was quickly injected into the reactor in less than 5 s. Samples were collected every 5 min at the tracer collection point for at least twice during the designed hydraulic retention time (HRT). Each sample was filtered to reduce the interference of solids. Mass balances were performed on the effluent data series so as to calculate tracer recovery percentages. The measurement of the fluoride concentrations was carried out through the fluoride ion-selective electrode.

Grid (Time=3.2648e+05)   Sep 16, 2009
                    FLUENT 6.3 (3d, pbns, lam, unsteady)
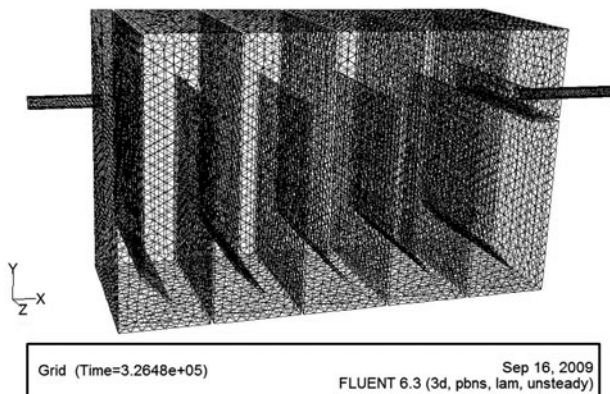
Fig. 2. Computational grids in a 5-compartment ABR model.

3. Theoretical analyses

Eq. (1) was used to calculate $E(t)$, T,

$$E(t) = \frac{C(t)}{\int_0^\infty C(t)\mathrm{d}t} \tag{1}$$

The mean residence time $\bar{t}$,

$$\bar{t} = \frac{\int_0^\infty tE(t)\mathrm{d}t}{\int_0^\infty E(t)\mathrm{d}t} \tag{2}$$

Variance of RTD σ_t^2

$$\sigma_t^2 = \int_0^\infty t^2 E(t)\mathrm{d}t - (\bar{t})^2 \tag{3}$$

where t is the time, T; $C(t)$ is the tracer concentration at time t, ML^{-3}.

The axial dispersion model was used when the degree of back-mixing was relatively low [38,39], as it is assumed that under such circumstances the back-mixing occurs only in the axial direction while that in the radial direction can be neglected.

Further, assuming that both the substrate concentration across the bed diameter and the fluid velocity maintained constant, applying Fick's law in the axial (l) direction, considering the reactor under stable state, the axial dispersion model can be easily established as follows [29,36]:

$$\frac{\partial C(t)}{\partial t} = D\frac{\partial^2 C(t)}{\partial l^2} - u\frac{\partial C(t)}{\partial l} \tag{4}$$

where l represents the axial distance of the reactor, L; D is the axial dispersion coefficient, L^2/T; u is the flow rate, L/T. If dimensionless concentration $C^* = C / C_0$ (C_0 was the initial tracer concentration, ML^{-3}), dimensionless time $\theta = t/\bar{t}$, and dimensionless length $Z = l/L$ (L is the length of the reactor, L, l is a point along the

reactor, $0 < l < L$) were used, then the Eq. (4) was changed to:

$$\frac{\partial C^*(\theta)}{\partial \theta} = (D/uL)\frac{\partial^2 C^*(\theta)}{\partial Z^2} - u\frac{\partial C^*(\theta)}{\partial Z} \tag{5}$$

where D/uL is the dispersion number (dimensionless). The dispersion number could characterize the degree of back-mixing in the flow direction. The bigger was the number, the stronger was the back-mixing. When $D/uL > 0.01$, by solving and rearranging the partial differential Eq. (5), we obtained:

$$\sigma_\theta^2 = 2\left(\frac{D}{uL}\right) - 2\left(\frac{D}{uL}\right)^2\left(1 - e^{-uL/D}\right) \tag{6}$$

where σ_θ^2 is the dimensionless variance of the $\sigma_\theta^2 = \sigma_t^2/t^2$ and the RTD. Therefore, D/uL could be calculated using Eqs. (1) and (4). If $D/uL = 0$, the reactor approximated to the ideal plug-flow reactor (PFR, $D/uL = 0$). If $D/uL = \infty$, the reactor approximated to the ideal continuous-flow stirred-tank reactor (CSTR, $D/uL = 1$). In case of non-ideal flow, D/uL value was between 0 and 1 ($0 < D/uL < 1$).

The tank-in-series model was applied when the degree of back-mixing was relatively strong [24,38]. Under such circumstances, the variation rate of the tracer concentration in an infinitesimal volume was demonstrated as:

$$C(t) = \frac{C_0}{(N-1)!}\left(\frac{t}{\tau}\right)^{(N-1)} e^{-t/\tau} \tag{7}$$

where τ is the HRT for each reactor, T; N is the series number.

The σ_θ^2 in Eq. (7) was:

$$\sigma_\theta^2 = \int_0^\infty \frac{N^N \theta^{N+1} e^{-N\theta}}{(N-1)!} d\theta - 1 = \frac{1}{N} \tag{8}$$

Rearranging Eq. (8), we obtained:

$$N = \frac{1}{\sigma_\theta^2} \tag{9}$$

Therefore, N as a main parameter of the tank-in-series model could be calculated by Eq. (9). The tank-in-series model simulated the actual CSTR reactor with the same volume in series. If $N = 1$, then the reactor approximated to the CSTR, and if $N = \infty$, then the

reactor approximated to the PFR. Dead space of the reactor (V_d, %) could be calculated as follows:

$$V_d = (1 - \bar{t}/\text{HRT}) \times 100\% \tag{10}$$

4. Results and discussion

4.1. RTD of ABR

The RTD curves obtained through designed reactors and the physical model test were compared by means of the computational fluid dynamic model (Fig. 3). Through adjusting the parameters of the model simulation results to measured values with the relative error less than 20%, the parameter calibration was therefore accomplished. The model obtained in this way can be used for estimating the reaction flow field and the mixed flow pattern of the ABR.

Fig. 4 shows the RTD of 3-, 4-, 5-, and 6-compartment ABRs, respectively. As shown in the figure, the reactor residence time curve firstly rises and then drops, forming one single peak. The calculated peak concentrations of 3-, 4-, 5-, and 6-compartment ABRs were 1.68, 1.83, 2.09, and 2.38 mg/L, respectively. Further analysis of the RTD of 3-, 4-, 5-, and 6-compartment ABRs showed that, with the increase in the ABR compartments, the peak value of the RTD curves increased as well, while the distribution width of the RTD curves turned narrower on the time axis and the maximal concentration of the tracer appeared at the time point that was twice of the HRT. The analysis also found that the width of the RTD and the value of the maximal concentration of the tracer also slightly increased with the increase in the ABR compartment however, such an increase could be negligible.
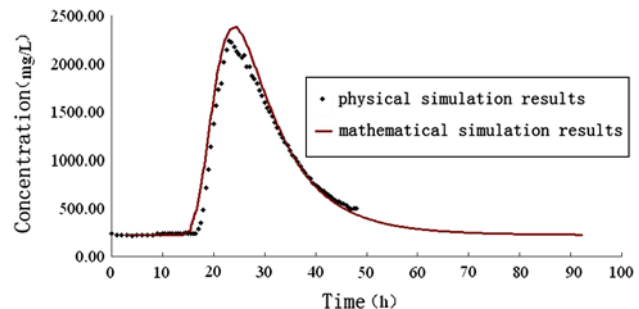
Fig. 3. RTD results obtained through mathematical simulation and physical simulation (based on the 5-compartment ABR model).
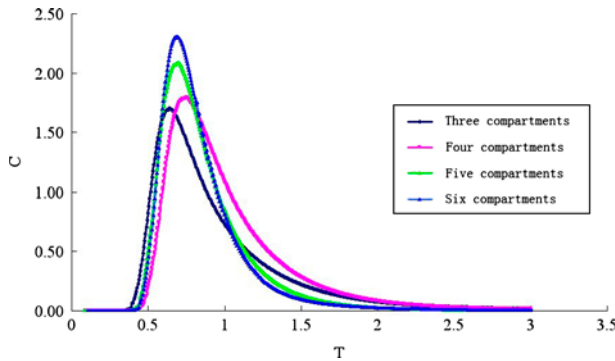
Fig. 4. RTD results of 3-, 4-, 5-, and 6-compartment ABRs (collected at the outlet).

4.2. Back-mixing in the ABR

Peclet number of quasi (Pez) is the ratio of the rate of the convective flow to the rate of the axial diffusion, which is often used to indicate the degree of back-mixing. When Pez tends 0 (namely, 1/Pez tends to ∞), the advection is much greater than the diffusion; that is to say, the fluid is completely in the form of mixed flow. On the contrary, when Pez tends to ∞, (namely, 1/Pez tends to 0), the influence of the diffusion upon the convection is negligible; that is to say, the fluid is in the form of plug flow.

Analysis of the hydraulic characteristics of 3-, 4-, 5-, and 6-compartment ABRs under the same operating conditions showed that, keeping the HRT value constant, the number of compartments had greater impact on the hydraulic characteristics of the ABR. The 1/Pez values of 3-, 4-, 5-, and 6-compartment ABRs were 0.118, 0.083, 0.061, and 0.060, respectively (Fig. 5). There was a great drop between the 1/Pez of the 3-compartment ABR and that of the 4-compartment ABR; while the difference between the 1/Pez of the 5-compartment ABR and that of the 6-compartment ABR was negligible.
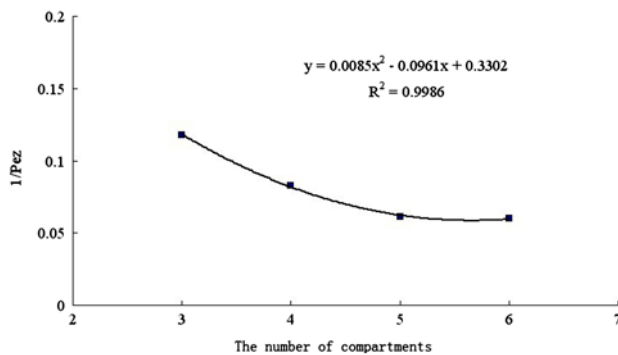
The 1/Pez of the 3-compartment ABR was twice as much as that of the 6-compartment ABR. Therefore, the plug flow pattern could be obtained in the reactor by increasing the number of compartments [38]. Tomlinson and Chambers found that when 1/Pez > 0.2, the degree of dispersion in the reactor was kept high. Likely, in this study, as the 1/Pez values of the four ABRs turned from 0.118 to 0.060, that of the 3-compartment ABR was the highest. Therefore, the fluid in the 3-compartment ABR tended to be in the form of complete mixed flow while that in the 6-compartment ABR tended to be in the form of plug flow.

As the 1/Pez value decreased, the fluid in the reactor gradually approached to the plug flow. That is to say, with the compartments increased from three to six, the fluid in the reactor increasingly took the form of plug flow.

4.3. Dead space in the ABR

Dead space in the reactor can be generally divided into hydraulic dead space and biomass dead space. As shown in Fig. 6 and Table 2, the increase in the compartments lead to the decrease in the percentage of hydraulic dead space (with reducing amplitude). The mean dead spaces, including that caused by biomass and hydraulic behavior, in 3-, 4-, 5-, and 6-compartment ABRs were 6.40, 5, 3.30, and 3%, respectively. The reducing ratios of dead space in the 3-compartment ABR to the 6-compartment ABR were 21.8, 34, and 10%, respectively. Though the dead space in the 6-compartment ABR was smaller than that in the 5-compartment ABR, the difference between them was much smaller than that between the 3-compartment ABR and the 4-compartment ABR, or that between the 4-compartment ABR and the 5-compartment ABR. Therefore, the optimal number of compartments of the reactor shall be 4 or 5.

Fig. 5. Percentages of dead space in 3-, 4-, 5-, and 6-compartment ABRs.
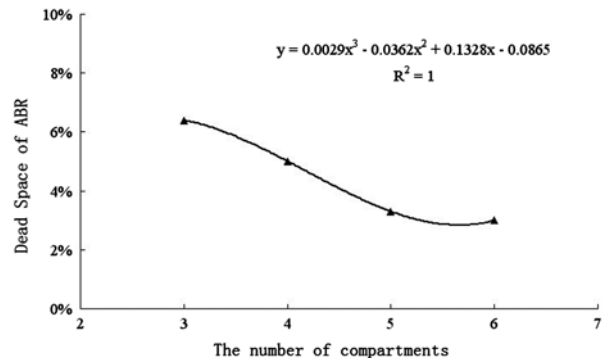
Fig. 6. 1/Pez of 3-, 4-, 5-, and 6-compartment ABRs.

Table 2
Working parameters of the ABR

ABR compartment index	HRT/h	σ_θ^2	N	1/Pez	Dead space
3-Compartment ABR	28.97	0.208	4.80	0.118	0.064
4-Compartment ABR	31	0.152	6.57	0.083	0.050
5-Compartment ABR	30.20	0.115	8.71	0.061	0.033
6-Compartment ABR	29.61	0.112	8.88	0.060	0.030

The hydraulic dead space in the ABR occurs mainly at the baffle corners and the weir outlets. The existence of vortex of various degrees at the baffle corners affects diffusion of the tracer, and consequently results in slow release of the tracer; the dead space is therefore formed. The percentage of dead space in an ABR with fewer compartments turns to be higher in that such a design causes comparatively larger retention area in the reactor due to the slow flow rate of fluid. In the present study, the mean dead spaces in 3-, 4-, 5-, and 6-compartment ABRs were 6.40, 5, 3.30, and 3%, respectively. As the number of reactor compartments increased from 3 to 6, the dead space in the reactor gradually diminished from 6.40% to 3%. It also confirmed that the hydraulic dead space occurred mainly at the baffle corners and the weir outlets, and the vortex which was formed therein hindered the diffusion of the tracer.

4.4. Volumetric efficiency of ABR

Providing that the reaction was a first-order reaction, and each tank had same volume and similar operational conditions, substrate conversion rate R, and series number N could be connected in the following equation:

$$R = 1 - (1 + k\tau)^{-N} \tag{11}$$

where k represents the reaction rate constant. Total volume of the reaction system could be calculated by the following equation:

$$V_N = NQ\tau = NQ\frac{1 - (1 - R)^{1/N}}{k(1 - R)^{1/N}} \tag{12}$$

where Q represents the influent flow rate, L^3/T. Assuming the total volume of N, CSTRs in series was V_N and the volume of single CSTR was V_1, the effect of flow pattern on the reactor volumetric efficiency could be reflected by the volume ratio of V_N and V_1 (V_N/V_1). When the same substrate conversion rate was required, the V_N/V_1 could be calculated by the following equation:

$$\frac{V_N}{V_1} = N \times \frac{1 - R}{R} \times \frac{1 - (1 - R)^{1/N}}{(1 - R)^{1/N}} \times 100\% \tag{13}$$

Assuming removal efficiency of 50% and 90%, and series number N 2, 3, … 7, according to formula (13), the formula (13) in series with series N derivative d(V_N/V_1)/dN, which is the volume change rate. Calculation results of V_N/V_1 and d(V_N/V_1)/dN were shown in Table 3.

As shown in Table 3, when the removal rate was kept at 50%, V_N/V_1 gradually decreased from 100% ($N = \infty$) to 69.31% ($N = 1$) with the increase in N, and the volume required for obtaining the ideal plug flow state was equivalent to 69.31% of the volume of the ideally complete mixed flow state. Similarly, when the removal rate was kept at 90%, V_N/V_1 decreased from 100% ($N = 1$) to 25.58% ($N = \infty$) with the increase in N, and the volume required for obtaining the ideal plug

Table 3
Relationship between the number of tank-in-series N and effective volume VN

N	1	2	3	4	5	6	7	∞
R	50%	50%	50%	50%	50%	50%	50%	50%
V_N/V_1	1	0.8284	0.7798	0.7568	0.7435	0.7348	0.7287	0.6931
d(V_N/V_1)/dN	–	–	0.0487	0.0229	0.0133	0.0087	0.0061	–
R	90%	90%	90%	90%	90%	90%	90%	90%
V_N/V_1	1	0.4805	0.3848	0.3459	0.3249	0.3119	0.3029	0.2558
d(V_N/V_1)/dN	–	–	0.0957	0.0389	0.0210	0.0131	0.0089	

flow state was only equivalent to 25.58% of the volume of the ideally complete mixed flow state. It can be concluded that higher the removal rate of the reactor system, larger the value of N was required, and the more likely reactor obtained the plug flow state.

In contrast, the N number in the present study was 4–6, slightly bigger than other reactor systems; consequently, the flow state therein was mostly a plug one. Therefore, the N number is an important reactor parameter. Sensitivity analysis of the N number will show its importance to a reactor system. The $d(V_N/V_1)/dN$ number of the model is shown in Table 3. We found that, when the N number was 1–4, it was comparatively more sensitive to the volumetric efficiency (V_N/V_1) of the reactor (the volumetric efficiency being 1, 0.8284, 0.7798, and 0.7568, respectively); however, when the N number was bigger than 4, V_N/V_1 value turned to be smaller (when the N value was set at 5, 6, 7, V_N/V_1 were 0.7435, 0.7348, 0.7287, respectively). In Ghaniyari–Benis et al. [40,41], two different kinetic models (one was based on a dispersion model with first-order kinetics for substrate consumption and the other was based on a modification of the Young equation) were evaluated and compared to predict the organic matter removal efficiency or fractional conversion. During their test, the first-order kinetic constant obtained with the dispersion model was 0.28 h^{-1} and the Peclet dispersion number was 45, with a mean relative error of 2%. The model based on the Young equation predicted the behavior of the reactor more accurately, showing deviations lower than 10% between the theoretical and experimental values of the fractional conversion—the mean relative error being 0.9% in this case. In contrast, most of researchers, including authors of this paper, adopted the axial dispersion model to simulate the flow state of a reactor system. Table 3 also showed that, when N increased to a certain value, the reducing amplitude of the effective volume of the reaction system narrowed down. When $d(V_N/V_1)/dN$ of a highly effective spiral anaerobic bioreactor was controlled at 1–4% or less, the series value N was $4 \le N \le 5$ when the removal rate was 50% and $4 \le N \le 6$ when the removal rate was 90%. Taking the operating performance and economic factors of the reactor into full consideration, this paper recommends that the series value N of the ABR shall be kept at 4 or 5.

5. Conclusions

The percentage of dead space in a reactor was negatively correlated to the number of ABR compartments. Specifically, the mean dead spaces caused by biomass and hydraulic behavior in 3-, 4-, 5-, and 6-compartment ABRs were 6.40, 5, 3.3, and 3%, respectively.

The negative correlation was also seen between the degree of back-mixing and the number of ABR compartments, with 1/Pez being 0.060–0.118. With the increase in compartments, the fluid in the reactor gradually approached to the ideal plug flow state. Analysis showed that the theoretically optimal number of ABR compartments (namely, the value of series number N) shall be kept at $4 \le N \le 5$ when the removal efficiency of the reaction system was 50% and $4 \le N \le 6$ when the removal efficiency of the reaction system was 90%. Taking the operating performance and economic factors of the reactor into full consideration, the series value N of the ABR compartments shall be kept at 4 or 5.

References

[1] X.G. Chen, Z. Ping, S. Ding, C.J. Tang, J. Cai, Specific energy dissipation rate for super-high-rate anaerobic bioreactor, J. Chem. Technol. Biotechnol. 86 (2011) 749–756.

[2] B. Demirel, O. Yenigun, T.T. Onay, Anaerobic treatment of dairy wastewaters: A review, Process Biochem. 40 (2005) 2583–2595.

[3] J. Lu, Y.f. Ma, Y.R. Liu, M.H. Li, Treatment of hypersaline wastewater by a combined neutralization–precipitation with ABR–SBR technique, Desalination 277 (2011) 321–324.

[4] M.X. Zheng, K.J. Wang, J.E. Zuo, Z. Yan, H. Fang, J.W. Yu, Flow pattern analysis of a full-scale expanded granular sludge bed-type reactor under different organic loading rates, Bioresour. Technol. 107 (2012) 33–40.

[5] A. Tawfik, A. Salem, M. El-Qelish, Two stage anaerobic baffled reactors for bio-hydrogen production from municipal food waste, Bioresour. Technol. 102 (2011) 8723–8726.

[6] W. Wang, L. Xie, J. Chen, G. Luo, Q. Zhou, Biohydrogen and methane production by co-digestion of cassava stillage and excess sludge under thermophilic condition, Bioresour. Technol. 102 (2011) 3833–3839.

[7] D.C. Rodríguez, M. Belmonte, G. Peñuela, J.L. Campos, G. Vidal, Behaviour of molecular weight distribution for the liquid fraction of pig slurry treated by anaerobic digestion, Environ. Technol. 32 (2011) 419–425.

[8] L. Seghezzo, G. Zeeman, J.B. van Lier, H.V.M. Hamelers, G. Lettinga, A review: The anaerobic treatment of sewage in UASB and EGSB reactors, Bioresour. Technol. 65 (1998) 175–190.

[9] S.H. Kim, H. Sun-Kee, S. Hang-Sik, Feasibility of bio-hydrogen production by anaerobic co-digestion of food waste and sewage sludge, Int. J. Hydrogen Energy 29 (2004) 1607–1616.

[10] Y.Z. Lin, J. Yin, J.H. Wang, W.D. Tian, Performance and microbial community in hybrid anaerobic baffled reactor-constructed wetland for nitrobenzene wastewater, Bioresour. Technol. 118 (2012) 128–135.

[11] D.B. Levin, L. Pitt, M. Love, Biohydrogen production: Prospects and limitations to practical application, Int. J. Hydrogen Energy 29 (2004) 173–185.

[12] F.Y. Chang, C.Y. Lin, Biohydrogen production using an up-flow anaerobic sludge blanket reactor, Int. J. Hydrogen Energy 29 (2004) 33–39.

[13] G. Lettinga, A.F.M. van Velsen, S.W. Hobma, W.J. de Zeeuw, A. Klapwijk, Use of the upflow sludge blanket (USB) reactor concept for biological wastewater treatment, Biotechnol. Bioeng. 22 (2980) 699–734.

[14] A. Bachmann, V.L. Beard, P.L. McCarty, Comparison of fixed-film reactors with a modified sludge blanket reactor, in: Proceedings of the First International Conference on Fixed-Film Biological Processes II, Kings Island, OH, 1982, pp. 1192–1211.

[15] A. Bachmann, V.L. Beard, P.L. McCarty, Performance characteristics of the anaerobic baffled reactor, Water Res. 19 (1985) 99–106.

[16] W.P. Barber, D.C. Stuckey, The use of the anaerobic baffled reactor (ABR) for wastewater treatment: A review, Water Res. 33 (1999) 1559–1578.

[17] S. Nachaiyasit, D.C. Stuckey, The effect of shock loads on the performance of an anaerobic baffled reactor (ABR), 1. Step changes in feed concentration at constant retention time, Water Res. 31 (1997) 2737–2746.

[18] I.V. Skiadas, G. Lyberatos, The periodic anaerobic baffled reactor, Water Sci. Technol. 38 (1998) 401–408.

[19] R. Boopathy, V.F. Larsen, E. Senior, Performance of anaerobic baffled reactor (ABR) in treating distillery waste water from a Scotch Whisky factory, Biomass 16 (1988) 133–143.

[20] S. Ghaniyari-Benis, R. Borja, S.A. Monemian, V. Goodarzi, Anaerobic treatment of synthetic medium-strength wastewater using a multistage biofilm reactor, Bioresour. Technol. 100 (2009) 1740–1745.

[21] S. Ghaniyari-Benis, R. Borja, M. Bagheri, S. Ali Monemian, V. Goodarzi, Z. Tooyserkani, Effect of adding nitrate on the performance of a multistage biofilter used for anaerobic treatment of high-strength wastewater, Chem. Eng. J. 156 (2010) 250–256.

[22] H.F. Wu, S.H. Wang, H.L. Kong, T.T. Liu, M.F. Xia, Performance of combined process of anoxic baffled reactor-biological contact oxidation treating printing and dyeing wastewater, Bioresour. Technol. 98 (2011) 1501–1504.

[23] Z.B. Chen, M.H. Cui, N.Q. Ren, Z.Q. Chen, H.C. Wang, S.K. Nie, Improving the simultaneous removal efficiency of COD and color in a combined HABMR–CFASR system based MPDW. Part 1: Optimization of operational parameters for HABMR by using response surface methodology, Bioresour. Technol. 102 (2011) 8839–8847.

[24] J. Lu, Y.F. Ma, Y.R. Liu, M.H. Li, Treatment of hypersaline wastewater by a combined neutralization precipitation with ABR–SBR technique, Desalination 277 (2011) 321–324.

[25] Y.Z. Lin, J. Yin, J.H. Wang, W.D. Tian, Performance and microbial community in hybrid anaerobic baffled reactor-constructed wetland for nitrobenzene wastewater, Bioresour. Technol. 118 (2012) 128–135.

[26] A. Tawfik, M. El-Qelish, Continuous hydrogen production from co-digestion of municipal food waste and kitchen wastewater in mesophilic anaerobic baffled reactor, Desalination 114 (2012) 270–274.

[27] I.K. Kapdan, F. Kargi, Bio-hydrogen production from waste materials, Enzyme Microb. Technol. 38 (2006) 569–582.

[28] M.L. Chong, V. Sabaratnam, Y. Shirai, M.A. Hassan, Biohydrogen production from biomass and industrial wastes by dark fermentation, Int. J. Hydrogen Energy 34 (2009) 3277–3287.

[29] L.J. Burrows, A.J. Stokes, J.R. West, C.F. Forster, A.D. Martin, Evaluation of different analytical methods for tracer studies in aeration lanes of activated sludge plants, Water Res. 33 (1999) 367–374.

[30] X.G. Chen, P. Zheng, Y.J. Guo, Q. Mahmood, C.J. Tang, S. Ding, Flow patterns of super-high-rate anaerobic bioreactor, Bioresour. Technol. 101 (2010) 7731–7735.

[31] M. Terashima, R. Goel, K. Komatsu, H. Yasui, H. Takahashi, Y.Y. Li, CFD simulation of mixing in anaerobic digesters, Bioresour. Technol. 100 (2009) 2228–2233.

[32] A. Keshtkar, B. Meyssami, G. Abolhamd, H. Ghaforian, M. Khalagi Asadi, Mathematical modeling of non-ideal mixing continuous flow reactors for anaerobic digestion of cattle manure, Bioresour. Technol. 87 (2003) 113–124.

[33] I. Capela, M.J. Bilé, F. Silva, H. Nadais, A. Prates, L. Arroja, Hydrodynamic behaviour of a full-scale anaerobic contact reactor using residence time distribution technique, J. Chem. Technol. Biotechnol. 84 (2009) 716–724.

[34] J.Y. Ji, K. Zheng, Y.J. Xing, P. Zheng, Hydraulic characteristics and their effects on working performance of compartmentalized anaerobic reactor, Bioresour. Technol. 116 (2012) 47–52.

[35] A. Grobicki, D.C. Stuckey, Performance of the anaerobic baffled reactor under steady state and shock loading conditions, Biotechnol. Bioeng. 37 (1991) 344–355.

[36] Y. Jeffrey Yang, J.A. Goodrich, R.M. Clark, S.Y. Li, Modeling and testing of reactive contaminant transport in drinking water pipes: Chlorine response and implications for online contaminant detection, Water Res. 42 (2008) 1397–1412.

[37] A. Grobicki, D.C. Stuckey, Hydrodynamic characteristics of the anaerobic baffled reactor, Water Res. 26 (1992) 371–378.

[38] E.J. Tomlinson, B. Chambers, The Effect of Longitudinal Mixing on the Settleability of Activated Sludge, Technical Report TR 122, Stevenage, England, 1979.

[39] G. Lu, P. Zheng, Flow model of internal-loop granular sludge bed nitrifying reactor, Chin. J. Biotechnol. 19 (2003) 774–777 (in Chinese).

[40] S. Ghaniyari-Benis, A. Martín, R. Borja, Comparison of two mathematical models for correlating the organic matter removal efficiency with hydraulic retention time in a hybrid anaerobic baffled reactor treating molasses, Bioprocess. Biosyst. Eng. 35 (2012) 389–397.

[41] S. Ghaniyari-Benis, A. Martín, R. Borja, Kinetic modelling and performance prediction of a hybrid anaerobic baffled reactor treating synthetic wastewater at mesophilic temperature, Process Biochem. 45 (2010) 1616–1623.